



AD-A227 674

OFFICE OF NAVAL RESEARCH

Contract N00014-82K-0612

Task No. NR 627-838

TECHNICAL REPORT NO. 54

Investigations of the O<sub>2</sub> Reduction Reaction at the  
Platinum/Nafion Interface Using a Solid State  
Electrochemical Cell

by

<sup>a</sup>Arvind Parthasarathy, <sup>b</sup>Charles R. Martin, and  
<sup>c</sup>Supramaniam Srinivasan

Prepared for publication

in

Journal of the Electrochemical Chemical Society

<sup>a</sup>Department of Chemistry  
Texas A&M University  
College Station, TX 77843

<sup>b</sup>Department of Chemistry  
Colorado State University  
Ft. Collins, CO 80523

<sup>c</sup>Center for Electrochemical Systems & Hydrogen Research  
Texas A&M University  
College Station, TX 77843

September 25, 1990

Reproduction in whole or in part is permitted for  
any purpose of the United States Government

\*This document has been approved for public release  
and sale; its distribution is unlimited

\*This statement should also appear in Item 10 of Document  
Control Data - DD Form 1473. Copies of form  
Available from cognizant contract administrator

## REPORT DOCUMENTATION PAGE

Form Approved  
OMB No. 0704-0188

1a. REPORT SECURITY CLASSIFICATION UNCLASSIFIED			1b. RESTRICTIVE MARKINGS		
2a. SECURITY CLASSIFICATION AUTHORITY			3. DISTRIBUTION / AVAILABILITY OF REPORT APPROVED FOR PUBLIC DISTRIBUTION, DISTRIBUTION UNLIMITED.		
2b. DECLASSIFICATION / DOWNGRADING SCHEDULE					
4. PERFORMING ORGANIZATION REPORT NUMBER(S)  ONR TECHNICAL REPORT #54			5. MONITORING ORGANIZATION REPORT NUMBER(S)		
6a. NAME OF PERFORMING ORGANIZATION Dr. Charles R. Martin Department of Chemistry		6b. OFFICE SYMBOL (If applicable)	7a. NAME OF MONITORING ORGANIZATION Office of Naval Research		
6c. ADDRESS (City, State, and ZIP Code) Colorado State University Ft. Collins, CO 80523			7b. ADDRESS (City, State, and ZIP Code) 800 North Quincy Street Arlington, VA 22217		
8a. NAME OF FUNDING / SPONSORING ORGANIZATION Office of Naval Research		8b. OFFICE SYMBOL (If applicable)	9. PROCUREMENT INSTRUMENT IDENTIFICATION NUMBER Contract # N00014-82K-0612		
8c. ADDRESS (City, State, and ZIP Code) 800 North Quincy Street Arlington, VA 22217			10. SOURCE OF FUNDING NUMBERS		
			PROGRAM ELEMENT NO.	PROJECT NO.	TASK NO.
					WORK UNIT ACCESSION NO.
11. TITLE (Include Security Classification) Investigations of the O <sub>2</sub> Reduction Reaction at the Platinum/Nafion Interface Using a Solid State Electrochemical Cell					
12. PERSONAL AUTHOR(S) Arvind Parthasarathy and Charles R. Martin					
13a. TYPE OF REPORT Technical		13b. TIME COVERED FROM _____ TO _____		14. DATE OF REPORT (Year, Month, Day) (90, 09, 25) Sept. 25, 1990	
15. PAGE COUNT					
16. SUPPLEMENTARY NOTATION					
17. COSATI CODES			18. SUBJECT TERMS (Continue on reverse if necessary and identify by block number)		
FIELD	GROUP	SUB-GROUP	O <sub>2</sub> reduction kinetics, solid state electrochemistry, ultramicroelectrodes.		
19. ABSTRACT (Continue on reverse if necessary and identify by block number) Research in solid polymer electrolyte fuel cells is gaining momentum because of the prospects of attaining high energy efficiencies and power densities, essential for transportation and space applications. The most advanced solid polymer electrolytes for these fuel cells are the perfluorosulfonate ionomers (PFSIs) such as duPont's Nafion and the Dow PFSIs. The high oxygen solubility, chemical stability, proton conductivity and perselectivity exhibited by Nafion and the Dow PFSI's make them ideal candidates as electrolytes for fuel cells. Furthermore, the minimal anion adsorption on electrodes from fluorinated acids enhances oxygen reduction kinetics. The objectives of this work were to determine the concentration and diffusion coefficient of oxygen in Nafion, and the electrode kinetic parameters for the reduction of oxygen at the Pt/Nafion interface under totally solid state conditions (i.e. no contacting liquid electrolyte phase). Cyclic voltammetric and potentiostatic transient measurements were made at the Pt/Nafion interface. From cyclic voltammetric and potentiostatic transient measurements were made at the Pt/Nafion interface. From cyclic					
20. DISTRIBUTION / AVAILABILITY OF ABSTRACT <input type="checkbox"/> UNCLASSIFIED/UNLIMITED <input type="checkbox"/> SAME AS RPT. <input type="checkbox"/> DTIC USERS			21. ABSTRACT SECURITY CLASSIFICATION		
22a. NAME OF RESPONSIBLE INDIVIDUAL			22b. TELEPHONE (Include Area Code)		22c. OFFICE SYMBOL

19. cont.

voltammetric measurements, the purity of Nafion was ascertained and the roughness factor of the electrode was calculated. The slow sweep experiments yielded the Tafel parameters for oxygen reduction. From the two-section Tafel plot, the calculated exchange current densities were found to be higher than those obtained at any other Pt/acid interface. From an analysis of the potentiostatic transients, the calculated values of oxygen solubility and diffusion coefficient in Nafion were higher than previously reported. These differences in mass transfer data were attributed to differences in water content of the Nafion membrane.

Accession For	
NTIS CRA&I	<input checked="checked" type="checkbox"/>
DTIC TAB	<input type="checkbox"/>
Unannounced	<input type="checkbox"/>
Justification	
By	
Distribution/	
Availability Codes	
and/or	
Special	
A-1	



INVESTIGATIONS OF THE O<sub>2</sub> REDUCTION REACTION AT THE  
PLATINUM/NAFION® INTERFACE USING A SOLID STATE  
ELECTROCHEMICAL CELL

Arvind Parthasarathy\* & Charles R. Martin\*\*†

Department of Chemistry,  
Texas A & M University, College Station, Texas 77843.

Supramaniam Srinivasan†

Center for Electrochemical Systems & Hydrogen Research,  
Texas A&M University, College Station, Texas 77843.

O<sub>2</sub> reduction kinetics  
solid state electrochem-  
istry, ultramicro-  
electrodes.

® Nafion is a registered trademark of du Pont de Nemours Company.

\*\* To whom correspondence should be addressed.  
Present address: Department of Chemistry, Colorado State University,  
Fort Collins, Colorado - 80523.

\* Electrochemical Society Student Member

† Electrochemical Society Active Member

## **ABSTRACT**

Research in solid polymer electrolyte fuel cells is gaining momentum because of the prospects of attaining high energy efficiencies and power densities, essential for transportation and space applications. The most advanced solid polymer electrolytes for these fuel cells are the perfluorosulfonate ionomers (PFSIs) such as duPont's Nafion and the Dow PFSIs. The high oxygen solubility, chemical stability, proton conductivity and permselectivity exhibited by Nafion and the Dow PFSI's make them ideal candidates as electrolytes for fuel cells. Furthermore, the minimal anion adsorption on electrodes from fluorinated acids enhances oxygen reduction kinetics. The objectives of this work were to determine the concentration and diffusion coefficient of oxygen in Nafion, and the electrode kinetic parameters for the reduction of oxygen at the Pt/Nafion interface under totally solid state conditions (i.e. no contacting liquid electrolyte phase). Cyclic voltammetric and potentiostatic transient measurements were made at the Pt/Nafion interface. From cyclic voltammetric measurements, the purity of Nafion was ascertained and the roughness factor of the electrode was calculated. The slow sweep experiments yielded the Tafel parameters for oxygen reduction. From the two-section Tafel plot, the calculated exchange current densities were found to be higher than those obtained at any other Pt/acid interface. From an analysis of the potentiostatic transients, the calculated values of oxygen solubility and diffusion coefficient in Nafion were higher than previously reported. These differences in mass transfer data were attributed to differences in water content of the Nafion membrane.

## INTRODUCTION

In recent years, considerable interest has been shown in the development of high power density fuel cells for space and terrestrial applications. The solid polymer electrolyte fuel cell shows great promise as a reliable power source for such applications (1). The solid polymer electrolyte of choice, for the solid polymer electrolyte fuel cell, has been the perfluorosulfonate ionomer, Nafion® (2).

The study of half-cell reactions at the electrode/electrolyte interface is an important part of fuel cell research (3). In the more conventional phosphoric acid fuel cells, such fundamental studies have, for example, identified the causes for the kinetic limitations of the O<sub>2</sub> reduction reaction (4). We have recently described results of fundamental investigations of the O<sub>2</sub> reduction reaction at the Pt/Nafion interface. Nafion film-coated electrodes were used in these studies (5,6); however, the Pt/Nafion electrode was immersed in H<sub>2</sub>SO<sub>4</sub> or H<sub>3</sub>PO<sub>4</sub> solution during the analysis. Very little work of this type has been done at the solid state Pt/Nafion interface (i.e. in the absence of a contacting liquid electrolyte phase). In a study by one of us, (7) a Pt gauze electrode coated with Nafion was kept in contact with a Nafion membrane to carry out electrochemical investigations. However, because of high contributions from mass transport and ohmic overpotential, it was necessary to carry out a computer analysis to extract the electrode kinetic parameters. The objectives of this study were to minimize mass transport and ohmic effects. Our present experiments would mimic the conditions extant in the solid polymer electrolyte fuel cell.

We have designed a novel solid state electrochemical cell which allows for investigations of electrochemical processes occurring at the Pt/Nafion interface in the absence of a contacting electrolyte phase. We have used this cell to investigate the kinetics of O<sub>2</sub> reduction at the solid state Pt/Nafion interface. We have also determined the solubility and diffusion coefficient of O<sub>2</sub> in the solid state Nafion membrane. The results of these investigations are described here.

## **EXPERIMENTAL**

**Materials and Equipment.**— The solid polymer electrolyte was a 175  $\mu$ m-thick Nafion film (H<sup>+</sup>-form, 1100 Equivalent weight, du Pont). As-received Nafion membrane has a faint yellow coloration, usually ascribed to organic impurities (8). The cleaning procedure described below rendered the film transparent. The membrane was first cleaned for 30 minutes in boiling 3% hydrogen peroxide (Aldrich) to remove organics. The membrane was then immersed in hot (80 °C), quartz-distilled, 9M nitric acid (Seastar Chemicals) for 15 to 30 minutes. The Nafion was then rinsed in boiling MilliQ<sup>®</sup> water (Millipore Corp), sonicated in several aliquots of hot (90 °C) water and stored under water. The water in which it was stored was replaced daily. The bathing gases, nitrogen and oxygen, were of ultra-high purity grade (Matheson) and were used without further purification.

Electrochemical measurements were conducted using a PAR 273 potentiostat (EG & G, Princeton, NJ), in conjunction with an X-Y recorder (SE 780, BBC). The PAR 273 was driven by an IBM personal computer (5). Open circuit potential measurements were made with a Metex M-3650

digital voltmeter. Humidity and temperature measurements were made with a combination probe (RH 130, Omega) attached to a digital readout. **Electrodes.**— The working electrode was a 100  $\mu\text{m}$ -diameter platinum wire (Aesar), sealed in a 3 mm i.d. heavy-walled capillary tube. As indicated in Figure 1, the sealed end of the capillary was flared to provide a larger surface area. Electrical contact with the microelectrode was made with Woods' metal (Johnson Matthey). The bore of the capillary was sealed with Torr-Seal® (Varian Associates) epoxy (Figure 1). The working electrode face was polished with 600 grit carborundum paper and then with 10  $\mu\text{m}$ , 0.3  $\mu\text{m}$  and 0.05  $\mu\text{m}$  alumina (Buehler). The electrode was then sonicated in 1:1 reagent grade nitric-sulfuric acid mixture and rinsed in several portions of water.

The reference electrode was a solid-state version of the dynamic hydrogen electrode (DHE) (9). In the DHE, hydrogen and oxygen are electrolytically generated at two platinum electrodes in contact with an aqueous protic medium. In our case, the Nafion membrane served as the protic medium.  $\text{H}_2$  and  $\text{O}_2$  were generated by applying a current of 10  $\text{mA}/\text{cm}^2$  to the platinum wires by means of a 9 V battery connected in series with a 5.1  $\text{M}\Omega$  resistor (Figure 2). The hydrogen evolving electrode was then used as the reference electrode (9).

The DHE reference electrode was constructed as follows: Two 100  $\mu\text{m}$ -diameter platinum wires were sealed within a double-bore capillary (Wale Apparatus Company). The sealed end of the capillary was given a domed surface by preferentially polishing the periphery. The 100  $\mu\text{m}$ -diameter platinum disc electrodes were then platinized by galvanostatic cathodic deposition from a 20 mM chloroplatinic acid bath. Plating was continued until both platinum discs were coated with black deposits of colloidal platinum.



The counter electrode consisted of a perforated platinum foil (Aesar) (5 mm x 8 mm x 0.254 mm) spot-welded to a glass-sealed, 0.5 mm-diameter platinum wire (Figure 1). Both reference and counter electrodes were coated with a thin layer of Nafion (10). The Nafion coating improved contact with the Nafion solid polymer electrolyte membrane. As indicated in Figure 1, the solid polymer electrolyte is sandwiched between the working electrode assembly and the counter electrode assembly. The bathing gas accesses the solid polymer electrolyte via the perforations in the counter electrode.

**Cell Design Criteria.**— Electrochemical cells usually employ liquid electrolytes. However, in the last few years, electrochemical cells based on solid electrolytes have been described (11). Because solid electrolytes usually have lower conductivities than liquid electrolytes, these new solid state cells suffer from problems associated with uncompensated electrolyte resistance. This problem can be minimized by using a microelectrode as the working electrode in the solid state cell.

In addition to overcoming problems associated with high electrolyte resistance, the solid state cell, for these studies, must also allow for equilibration of the electrolyte membrane with oxygen or other bathing gases. Furthermore, provisions for varying the partial pressure, humidity, and the temperature of these gases must be designed into the cell. We have addressed all of these design criteria in our solid state electrochemical cell, shown in Figure 2.

The apparatus in Figure 2 consists of two Teflon plates (8.5 cm-dia.) which are spaced apart by short (3.5 cm) Kel-F columns. The upper plate houses the reference and counter electrodes. The lower plate houses the working electrode. The plates are held together by 4 Allen screws.

Good contact between the electrodes and the Nafion membrane is obtained by advancing the working electrode with a brass screw assembly (Figure 2). A Kel-F spacer isolates the working electrode from the rotation of the screw so that the electrode merely translates upward when the screw is advanced. The counter electrode could be forced downward with a separate screw. A Teflon spacer was placed between the counter-electrode foil and the cell body to lend the foil mechanical support during compression. The spacer has a hole drilled through it for direct access of gas over the Nafion film covering the microelectrode. The reference electrode was forced against the Nafion film by spring pressure (Figure 2). The spring constant was 45 kgf/cm (Century Spring Corp). The solid length of the spring was chosen to prevent overtightening of the electrodes, when the electrodes were brought together in compression.

The ability to expose the Nafion membrane to the bathing gas was the final design criterion to be met. This was accomplished by enclosing the entire apparatus shown in Figure 2 in a gas-tight anodized aluminum enclosure. The metal casing also served as a Faraday cage which provided the necessary shielding against stray fields and electromagnetic interference (12). The cell assembly was rendered gas-tight using Teflon gaskets and Viton O-rings.

The bathing gas was humidified by bubbling the gas through a 20 cm water column in a gas bubbler. The flow rate of the humidified gas, entering the cell, was set at approximately 90 ml/minute. Higher flow rates caused excessive condensation within the cell enclosure due to the entrainment of water droplets in the gas stream. Lower flow rates resulted in drying out problems of the Nafion membrane due to the longer times

required to saturate the volume of gas within the cell enclosure. The gas was admitted via a 3-way valve (Nupro) which could switch between two gas connections (e.g. N<sub>2</sub> and O<sub>2</sub>). The humidity/ temperature combination probe was inserted into the enclosure through a gas-tight feedthrough. The experiments reported here were carried out at atmospheric pressure, 24.5±0.5 °C and 99.9% relative humidity.

**Electrochemical methods.**— The intent of the experiments described below was to determine the kinetic parameters for oxygen reduction at the solid state platinum/Nafion interface and to measure the diffusion coefficient (D) and the concentration (C) of oxygen in Nafion. The Nafion membrane was equilibrated with humidified O<sub>2</sub> for 26 hours, prior to analysis. It should be mentioned at the outset that both the diffusion coefficient and solubility of O<sub>2</sub> in Nafion are dependent on the water content of the membrane. The values measured here were obtained for membranes with high water contents (19±2 % w/w). Future studies will address the question of the effect of water content on O<sub>2</sub> transport, solubility, and reduction kinetics within Nafion and other PFSIs.

Cyclic voltammetry was also used to assess the cleanliness of the Nafion film. As was observed in our previous studies (5), prolonged scanning at 100 mV/s resulted in cleaner films, as evidenced by the better resolution of the platinum surface electrochemical processes. Cyclic voltammetry was also used to determine the electrochemically active surface area of the working electrode (5). Open circuit potential (rest potential) measurements were made periodically to check the cleanliness of the electrochemical system (13).

The exchange current density (14) and transfer coefficient (15) were measured using a slow scan voltammetric experiment. The data on the rising portion of the voltammogram (the kinetically controlled region) were analyzed via conventional Tafel analysis (16). The exchange current density can be obtained by extrapolation of the Tafel plot to the equilibrium potential and the transfer coefficient can be calculated from the Tafel slope.

The oxygen diffusion coefficient and concentration were determined using the chronoamperometric method described previously (5,17). Briefly, the O<sub>2</sub> reduction reaction is driven at the diffusion controlled rate by applying a potential step from an initial potential of 1.1 V to a final potential of 0.4 V. The current at the microelectrode of radius  $r$ , is then given by (17):

$$i = \frac{nF\pi^{1/2}D^{1/2}Cr^2}{t^{1/2}} + \pi nFDCr$$

The time window of the chronoamperometric experiment was chosen to maintain the diffusion layer within the thickness of the membrane. A time window, spanning from 0.07 to 10 seconds, was chosen. The resulting current-time transient was recorded and the data analyzed via  $i$  vs.  $t^{1/2}$  plots. The quantity  $D^{1/2}C$  was obtained from the slope of the  $i$  vs.  $t^{1/2}$  plot; the quantity  $DC$  was obtained from the intercept (5,17). Thus, both  $D$  and  $C$  can be obtained from a single experiment.

## **RESULTS AND DISCUSSION**

### **Electrochemical pretreatment of the platinum/Nafion**

**interface.**— Curve A in Figure 3 shows an initial cyclic voltammogram (CV) at the platinum electrode with the Nafion membrane equilibrated with N<sub>2</sub>. This initial CV does not show any of the features of platinum surface electrochemistry (18). As was the case with our earlier studies (in aqueous electrolytes (5)), repeated scanning caused the characteristic Pt electrochemical features to grow in (5); after 60 scans, the CV showed the hydrogen adsorption and desorption waves as well as the oxide reduction and formation waves (curve B in Figure 3).

### **Effect of clamping pressure on cyclic voltammograms.**—

Uncompensated solution resistance, in a conventional electrochemical cell, can cause a reduction wave to shift to more negative potentials.

Uncompensated resistance is also a potential problem in the solid state experiment. There is, however, an additional resistance term in the solid state electrochemical cell - the electrode-membrane contact resistance (19). This resistance term can be minimized by increasing the pressure applied to the electrode/membrane interface (19). We call this pressure the 'clamping pressure'.

The clamping pressure, in our solid state cell, is adjusted by two screws (Figure 2) which advance the working and counter electrodes into the membrane. The effect of the clamping pressure on the position of the oxide reduction wave was studied. It was seen that the wave shifts to less negative potentials as the clamping pressure is increased (i.e. as the contact resistance is decreased). The clamping pressure was increased until the oxide reduction wave showed no further positive shifts. The CV obtained

at these high clamping pressures (65 kgf/cm<sup>2</sup>) is shown in Figure 4. All of the Pt surface electrochemical features are clearly resolved (18).

**Determination of electrode roughness factors from cyclic voltammograms.**— The roughness factor is defined as the experimentally determined electrode area divided by the geometric area (5). The experimentally determined area was obtained by averaging the area under the hydrogen adsorption and desorption waves in Figure 4 (20). The double layer charging area was subtracted from the hydrogen adsorption area. Experimentally determined areas, geometric areas and roughness factors are shown in Table I. The roughness factors obtained in the solid state cell and in aqueous solution (0.7 M H<sub>3</sub>PO<sub>4</sub>) were nearly the same; this indicates that good membrane/electrode contact was achieved in the solid state cell.

**Rest potential measurements.**— The rest potential of the Pt working electrode was 0.810 V versus DHE when the membrane was equilibrated with N<sub>2</sub>. The rest potential increased to 0.965 V upon exposure of the membrane to O<sub>2</sub>. This is somewhat less than the rest potential of 1.0 V obtained when a Pt electrode is immersed in O<sub>2</sub>-saturated phosphoric acid. Appleby has shown that the rest potential in O<sub>2</sub>-saturated H<sub>3</sub>PO<sub>4</sub> is always less than 1.0 V if oxidizable impurities (e.g. organics) are present in the solution (21). The rest potential obtained at the solid state Pt/Nafion interface suggests that trace levels of impurities are still present in the Nafion membrane.

**Determination of Electrode Kinetic Parameters from slow scan O<sub>2</sub> reduction voltammograms.**— Curve A in Figure 5 shows the slow scan CV when the membrane is equilibrated with N<sub>2</sub>. Upon exposure to

O<sub>2</sub>, a near-steady state O<sub>2</sub>-reduction wave appears (curve B in Figure 5). The magnitude of the O<sub>2</sub>-reduction wave increases gradually with time. Curve C in Figure 5 was obtained 26 hours after initial exposure of the membrane to O<sub>2</sub>. No further changes in the O<sub>2</sub> reduction wave were observed after this 26-hour equilibration period. The hysteresis observed in these voltammograms is probably due to trace levels of organic contaminants in the Nafion membrane, which block the surface at the lower potentials and are oxidized at higher potentials.

Low scan rate voltammograms (2 mV/s) at O<sub>2</sub>-equilibrated Nafion were used to determine the kinetic parameters for O<sub>2</sub> reduction at the solid state platinum/Nafion interface. The kinetic parameters of interest here, are the exchange current density and the transfer coefficient. These kinetic parameters were obtained via Tafel analysis of the slow scan CV data. The method used (22) is described below. The 'steady state' response is typically obtained by measuring the current at long times (say, 10 minutes) at each potential. In our experiments, the shapes of the voltammograms obtained by the discrete step method were practically identical to the voltammograms obtained by the slow sweep technique.

The near-steady state voltammogram was obtained under O<sub>2</sub>-saturated conditions (curve C in Figure 5). Data points from the kinetically controlled region of the voltammogram were chosen for Tafel analysis. These data were corrected for mass-transport effects by calculating the parameter  $i/i_l$ , where  $i$  is the current density at any potential and  $i_l$  is the voltammetric limiting current density. A typical Tafel plot [ $E$  vs  $\log\{i/i_l\}$ ] of such data is shown in Figure 6. The Tafel plot shows two well-defined linear regions (correlation coefficients better than 0.98)

extending over 2 orders of magnitude in current density. The onset of diffusional effects are manifest as a sharp fall-off ( $E < 0.6\text{ V}$  vs DHE) in the mass transfer corrected Tafel plot (Figure 6). The values of the exchange current densities,  $i_0$ , were obtained by extrapolation of the Tafel line to the equilibrium potential,  $E_{eq}$ , for  $\text{O}_2$  reduction ( $1.23\text{ V}$  versus standard hydrogen electrode). It is interesting to note that Tafel plots with two linear segments showing slopes of  $-RT/F$  ( $-60\text{ mV/decade}$ ) and  $-2RT/F$  ( $-120\text{ mV/decade}$ ) have also been reported for the  $\text{O}_2$ -reduction reaction in perchloric and sulfuric acids (23,24). These variations in the Tafel slopes imply the influence of different adsorption isotherms (e.g. Langmuir, Temkin) and different rate determining steps over the potential ranges investigated (25). The cleanliness of the electrode surface and the purity of the electrolyte are also vital for obtaining reproducible values of the Tafel slope (21).

The exchange current density for  $\text{O}_2$  reduction at the platinum/Nafion interface corresponding to each Tafel slope (typically obtained) is shown in Table II. Exchange current densities with corresponding Tafel slopes for  $\text{O}_2$  reduction in other acid media are also shown in Table II. The exchange current density obtained in this work is the highest value for  $\text{O}_2$  reduction to be reported to date. The next highest exchange current density was obtained in trifluoromethane sulfonic acid (TFMSA), the anion of which does not adsorb to platinum (26). It is interesting to note that TFMSA is, in essence, a monomeric version of Nafion. The data shown in Table II indicate that the Nafion solid polymer electrolyte shows even less specific adsorption than TFMSA. The facile  $\text{O}_2$  reduction kinetics at the



solid state Pt/Nafion interface has important implications for the solid polymer electrolyte fuel cell (27).

The Tafel plot also provides the transfer coefficient,  $\alpha$ , for the O<sub>2</sub>-reduction reaction. While the transfer coefficient determines the reaction pathway (25), most discussions of reaction mechanism are usually based on the Tafel slope,  $b$ . The Tafel slope, is related to  $\alpha$  via slope,  $b = -2.303 RT/\alpha nF$ , where  $n$  is the number of electrons transferred in the rate determining step. Assuming that the first electron transfer is the rate determining step, ( $n=1$ ), (28) in the multistep O<sub>2</sub> reduction mechanism, the transfer coefficient is computed, as  $\alpha = 0.5$  for the region with the Tafel slope of  $-118 (\pm 1)$  mV/decade. The Tafel slope of  $-63 (\pm 2)$  mV/decade obtained at low current densities has been explained by a mechanism of O<sub>2</sub> reduction where the reaction involves an initial fast charge transfer step followed by a chemical step which is rate determining under Langmuir conditions (29). The first electron transfer step may be rate determining on an oxide covered surface (at the lower current densities) under Temkin adsorption conditions (30).

The Tafel plot in Figure 6 with two Tafel slopes is very similar to plots obtained with aqueous acid electrolytes such as H<sub>2</sub>SO<sub>4</sub>, HClO<sub>4</sub> (23,24,31) and TFMSA (26,30). A detailed interpretation of the Tafel slopes, in terms of adsorption isotherms, is possible. However, such an interpretation requires knowledge of the reaction order, with respect to oxygen and [H<sup>+</sup>] (23,30,32). Investigations of the O<sub>2</sub>-reduction reaction order are in progress and will be reported in a future article.

#### **Determination of mass transport parameters of O<sub>2</sub> in Nafion.—**

A typical current-time transient, associated with O<sub>2</sub> reduction, at the

platinum/Nafion interface, is shown in Figure 7. A typical  $i$  vs.  $t^{-1/2}$  plot for such data is shown in Figure 8. As indicated earlier, the slope of the plot yields the product  $D^{1/2}C$ , and the intercept yields the product  $DC$ , so that both  $D$  and  $C$  can be evaluated (12). The  $D$  and  $C$  data, obtained for  $O_2$  in Nafion, are shown in Table III .

It is interesting to compare the results obtained here with  $D$  and  $C$  values for  $O_2$  in Nafion which is in contact with an aqueous solution phase. For example, the  $D$  value for  $O_2$  in Nafion which is in contact with 0.7 M  $H_3PO_4$  is 2.7 times larger than the  $D$  obtained here (Table III (5)). However, the concentration of  $O_2$  in the solid state Nafion experiment is 7 times larger than the concentration obtained in the  $H_3PO_4$ -equilibrated membrane.

These differences are undoubtedly related to the difference in water content between the membranes studied here and the solution-cast films used in our previous studies. We have shown that solution-cast films imbibe more water than the as-received membranes (33). Water acts as a plasticizer in Nafion (33). Thus, the films in our previous studies were more highly plasticized than the membranes investigated here. This explains the lower diffusion coefficient observed in these studies.

The lower water content of the membrane in the present work will also affect the net concentration of  $O_2$  in the membrane (i.e. the moles of  $O_2$  divided by the total membrane volume). Because the membranes studied here have lower water contents than the solution-cast films (studied previously), the membrane in the current studies have smaller volumes. Furthermore, Lee and Rodgers (34) have shown that  $O_2$  is 5 times more soluble in the fluorocarbon domain of Nafion than in the aqueous domain.

If we assume that the fluorocarbon domains in the membranes studied here and the solution-cast films (5) are both saturated with O<sub>2</sub>, then the higher membrane volume in the solution-cast case accounts for the lower O<sub>2</sub> concentration.

The D and C values obtained by Ogumi et al (35), are also presented in Table III. Ogumi's investigations were also conducted on as-received membranes. The difference between Ogumi's values and our values for O<sub>2</sub> solubility and diffusion coefficient are again, probably associated with differences in water content in the membranes. The Nafion membrane used in Ogumi's work was used in a 'flooded' condition as the Nafion membrane was in contact with water on one side. In our case, the Nafion film was simply bathed by humidified gas. Studies on the dependence of diffusion coefficient and concentration of O<sub>2</sub> in Nafion on the humidity of the bathing O<sub>2</sub> gas are currently in progress.

## CONCLUSIONS

The mass transport parameters for O<sub>2</sub> in Nafion and the electrode kinetic parameters for O<sub>2</sub> reduction at the solid state platinum/Nafion interface were determined. These investigations were done in a novel solid state cell that overcomes ohmic limitations at the resistive interface. High exchange current densities were obtained for the O<sub>2</sub> reduction reaction due to lack of anionic adsorption effects from the electrolyte. Two Tafel slopes, -60 mV/decade and -120 mV/decade, (similar to those obtained at other Pt/acid interfaces) were obtained for oxygen reduction at the Pt/Nafion interface. The diffusion coefficient and the solubility of oxygen

in Nafion were higher than those reported previously. These results can be explained on the basis of the dependence of the mass transport parameters on the water content of the membrane.

## ACKNOWLEDGEMENTS

We would like to thank the Machine and Glass Shops of the Chemistry Department, Texas A&M University, for the expeditious completion of the fabrication of the components of the cell. We would also like to thank Drs. M.A. Enayetullah and A.J. Appleby for helpful discussions. This work was funded in part by Defense Advanced Research Projects Agency-Office of Naval Research, the Electric Power Research Institute and Energy Research in Applications Program-Texas Higher Education Co-ordinating Board.

## REFERENCES

1. S. Srinivasan, *This Journal*, **136**, 41C (1989).
2. A.B. Conti, A.R. Fragala and J.R. Boyack, *Proc. Electrochem. Soc.*, **77**, 354 (1977).
3. S. Srinivasan and J.O'M Bockris, "Fuel Cells: Their Electrochemistry", Chap.9, p. 469, McGraw Hill, New York (1969).
4. K.L. Hsueh, E.R. Gonzalez, S. Srinivasan, and D.T. Chin, *This Journal*, **131**, 823 (1984).
5. D.R. Lawson, L.D. Whiteley, C.R. Martin, M.N. Szentirmay, J.I. Song, *This Journal*, **135**, 2247 (1988).

6. S. Gottesfeld, I.D. Raistrick and S. Srinivasan, *This Journal*, **134**, 1455 (1987).
7. W. Paik, T.E. Springer and S. Srinivasan, *This Journal*, **136**, 644 (1989).
8. E.A. Ticianelli, C.R. Derouin and S. Srinivasan, *J. Electroanal. Chem.*, **251**, 275 (1988).
9. J. Giner, *This Journal*, **111**, 376 (1964).
10. C.R. Martin and K.A. Dollard, *J. Electroanal. Chem.*, **159**, 127 (1983).
11. L. Geng, R.A. Reed, M. Longmire and R.W. Murray, *J. Phys. Chem.*, **91**, 2908 (1987).
12. L.D. Whiteley and C.R. Martin, *J. Phys. Chem.*, **93**, 4650 (1989).
13. H. Wroblowa, M.L.B. Rao, A. Damjanovic and J.O'M. Bockris, *J. Electroanal. Chem.*, **15**, 139 (1967).
14. Reference 3, Chap.2, p. 67.
15. A.J. Bard and L.R. Faulkner, "Electrochemical Methods", Chap.3, p. 96, John Wiley, New York (1980).
16. K.J. Vetter, "Electrochemical Kinetics", Chap. 2, p.143, Academic Press, New York (1967).
17. C.P. Winlove, K.H. Parker, R.K.C. Oxenham, *J. Electroanal. Chem. Interfacial Electrochem.*, **170**, 293 (1984).
18. H. Angerstein-Kozłowska, B.E. Conway, W.B.A. Sharp, *J. Electroanal. Chem.*, **43**, 9 (1973).
19. Z. Cai, C. Liu and C.R. Martin, *This Journal*, **136**, 3356 (1989).
20. A.N. Frumkin, in "Advanced Electrochemistry," Vol. 3, P. Delahay, Editor, p.287, John Wiley & Sons, Inc., New York (1967).
21. A.J. Appleby, *This Journal*, **117**, 328, (1970).

22. S. Park, S. Ho, S. Aruliah, M.F. Weber, C.A. Ward, R.D. Venter and S. Srinivasan, *This Journal*, **133**, 1641 (1986).
23. A. Damjanovic and V. Brusic, *Electrochim. Acta*, **12**, 615 (1967).
24. A. Damjanovic and M.A. Genshaw, *Electrochim. Acta*, **15**, 1281 (1970).
25. A.C. Riddiford, *Electrochim. Acta*, **4**, 170 (1961).
26. M.A. Enayetullah, T.D. DeVilbiss and J.O'M Bockris, *This Journal*, **136**, 3369 (1989).
27. A.J. Appleby and E.B. Yeager in S.S. Penner(Ed.), *Assessment of Research Needs for Advanced Fuel Cells by the DOE AFCWG, Solid Polymer Electrolyte Fuel Cells*; Chap. 4, (1985).
28. D.B. Sepa, M.V. Vojnovic and A. Damjanovic, *Electrochim. Acta*, **26**, 781, (1981).
29. W.E. O'Grady and J. Zagal, Abstract 301, p.486, The Electrochemical Society Extended Abstracts, vol. 82-2, Detroit, MI, Oct.17-21, (1982).
30. A.J. Appleby and B.S. Baker, *This Journal*, **125**, 404 (1978).
31. A. Damjanovic, A. Dey, and J. O'M. Bockris, *Electrochim. Acta*, **11**, 791 (1966).
32. K.L. Hsueh, H.H. Chang, D.T. Chin and S. Srinivasan, *Electrochimica Acta*, **30**, 1137 (1985)
33. R.B. Moore and C.R. Martin, *Macromolecules*, **21**, 1334 (1988).
34. P.C. Lee and M.A.J. Rodgers, *J. Phys. Chem.*, **88**, 4385 (1984).
35. Z. Ogumi, Z. Takehara, S. Yoshizawa, *This Journal*, **131**, 769 (1984).

Table I. Pt working electrode roughness factors

Electrode/electrolyte interface	Experimentally determined area (cm <sup>2</sup> )	Geometric area (cm <sup>2</sup> )	Roughness factor
Pt/Nafion	$7.22 \times 10^{-4}$	$7.85 \times 10^{-5}$	9.2
Pt/H <sub>3</sub> PO <sub>4</sub>	$7.53 \times 10^{-4}$	$7.85 \times 10^{-5}$	9.6

Table II. Exchange current density at various platinum/electrolyte interfaces.

Electrolyte *	Tafel slope, b (mV/decade)	$i_0$ (A/cm <sup>2</sup> )†	References
Nafion membrane	-119	$7.8 \times 10^{-7}$	This work
	-63	$2.05 \times 10^{-9}$	
9.5 M TFMSA **	-118	$1.48 \times 10^{-7}$	(26)
6.0 M TFMSA	-61	$1.4 \times 10^{-8}$	(26)
1.1 N TFMSA	-60	$9 \times 10^{-11}$	(30)
0.1 N HClO <sub>4</sub>	-60	$8 \times 10^{-11}$	(23)
85% H <sub>3</sub> PO <sub>4</sub>	-60	$4 \times 10^{-13}$	(21)

\* T=298 K, p= 1atm O<sub>2</sub> except for \*\*;      \*\* T=308 K

† Exchange current density is calculated according to geometric area.



Table III: Diffusion coefficients and solubilities of oxygen in Nafion under various experimental conditions.

Parameter	Nafion solid polymer electrolyte (this work) <sup>a</sup>	Nafion immersed in water <sup>b</sup>	Nafion in H <sub>3</sub> PO <sub>4</sub> <sup>c</sup>
Diffusion coefficient, D cm <sup>2</sup> /s	7.4 (±0.3) × 10 <sup>-7</sup>	2.4 × 10 <sup>-7</sup>	2 × 10 <sup>-6</sup>
Concentration, C mM	26(± 1)	7.2	3.8

a. Temp. = 25 °C

b. Temp. = 30 °C, ref. 35

c. ref. 5

## List of Figures

- Figure 1: A simplified schematic of the solid state cell.
- Figure 2: A detailed schematic showing the individual components of the solid state cell.
- Figure 3: Initial CVs shown (A and B) at the Pt/Nafion interface recorded at  $100 \text{ mVs}^{-1}$ .
- Figure 4: CV at high clamping pressure: 26 hours of cycling after  $\text{N}_2$  blanketed the cell, scan rate= $100 \text{ mVs}^{-1}$ .
- Figure 5: Slow scan ( $2 \text{ mVs}^{-1}$ ) CVs for  $\text{O}_2$  reduction.
- Figure 6: Mass transfer corrected Tafel plot obtained for  $\text{O}_2$ -reduction at the Pt/Nafion interface.
- Figure 7: Current-time transient for  $\text{O}_2$ -reduction at the Pt/Nafion interface.
- Figure 8: Current vs.  $t^{-1/2}$  plot for  $\text{O}_2$ -reduction at the Pt/Nafion interface.

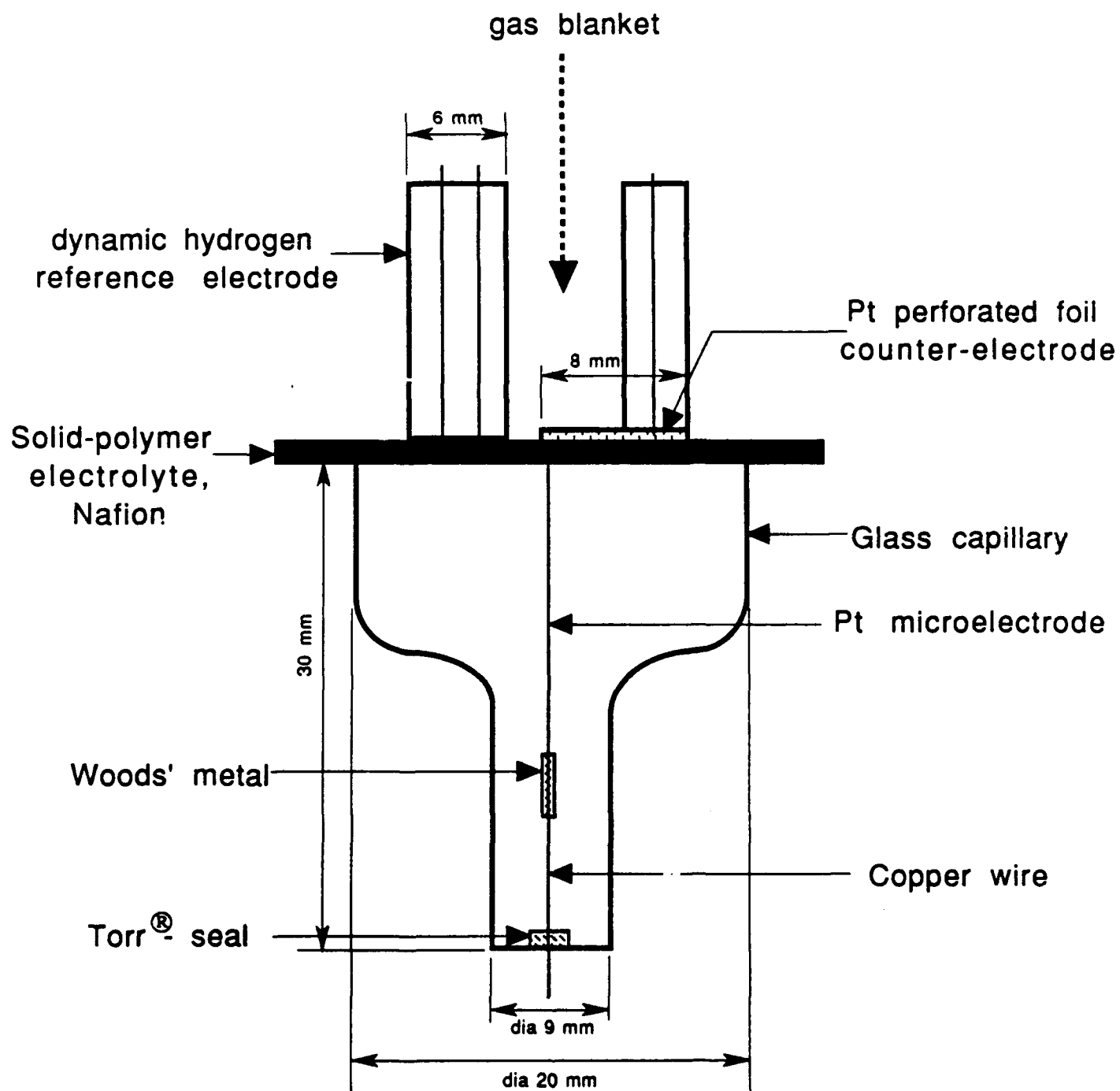


Figure 1

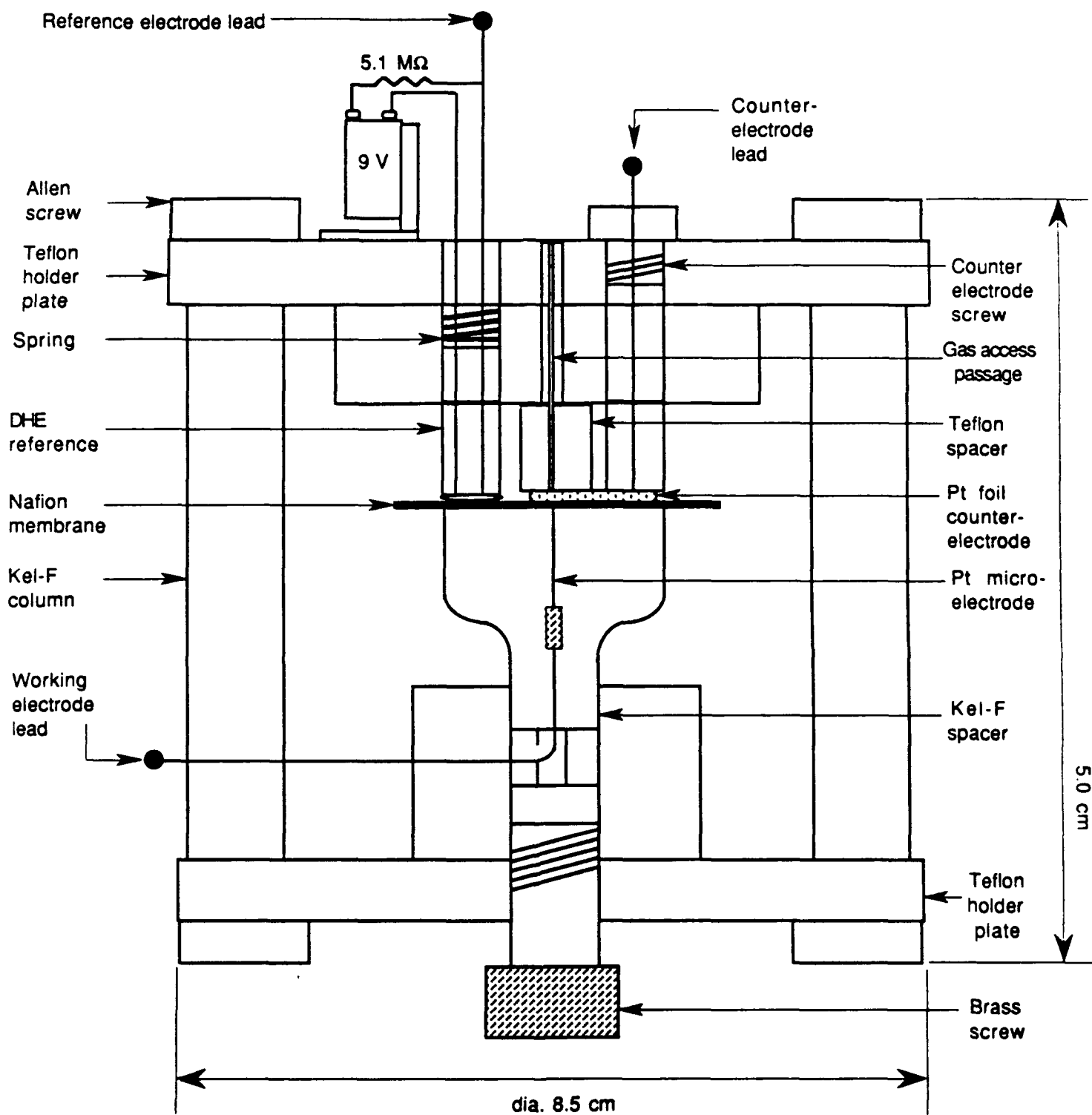


Fig. 2

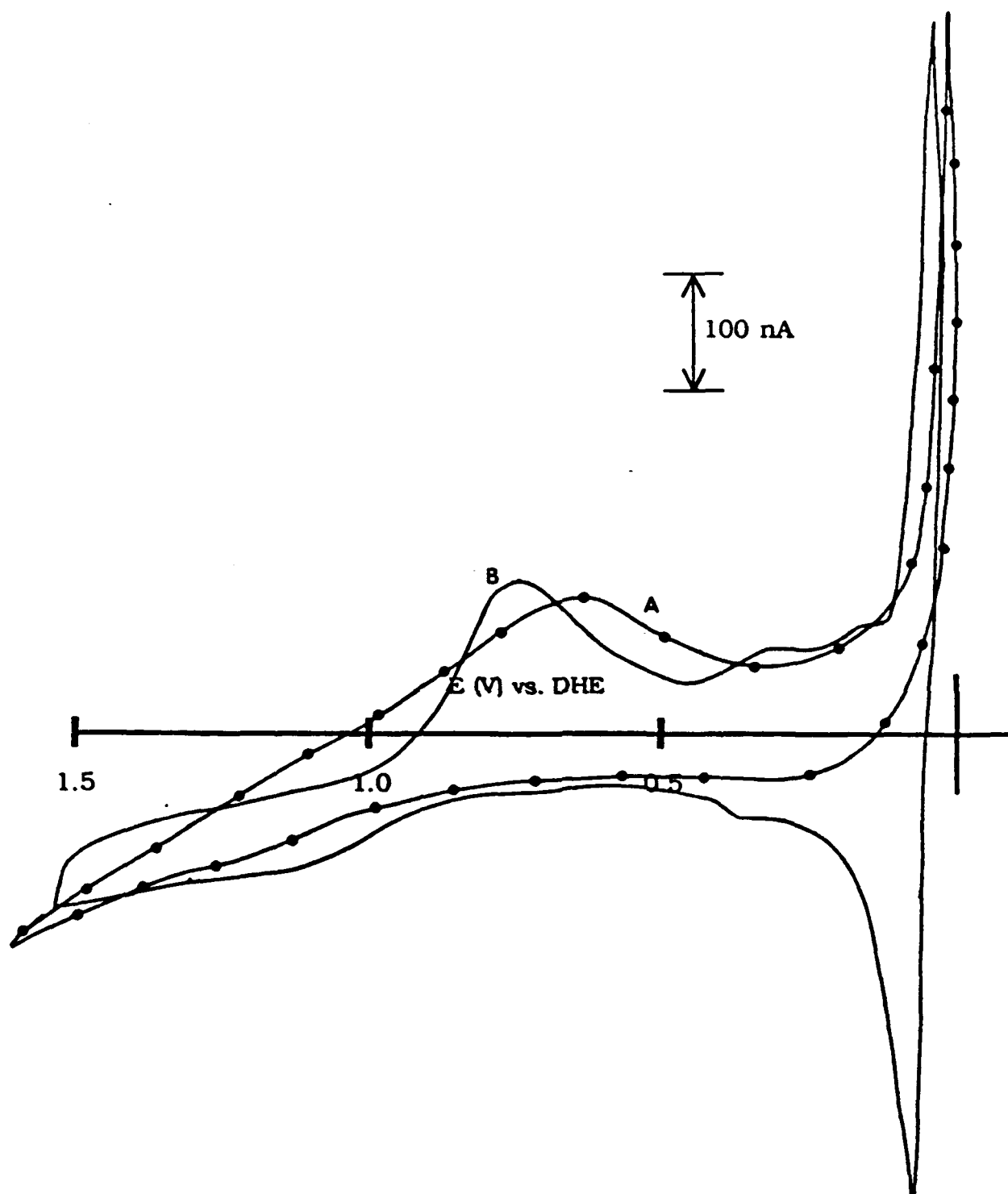


Figure 3

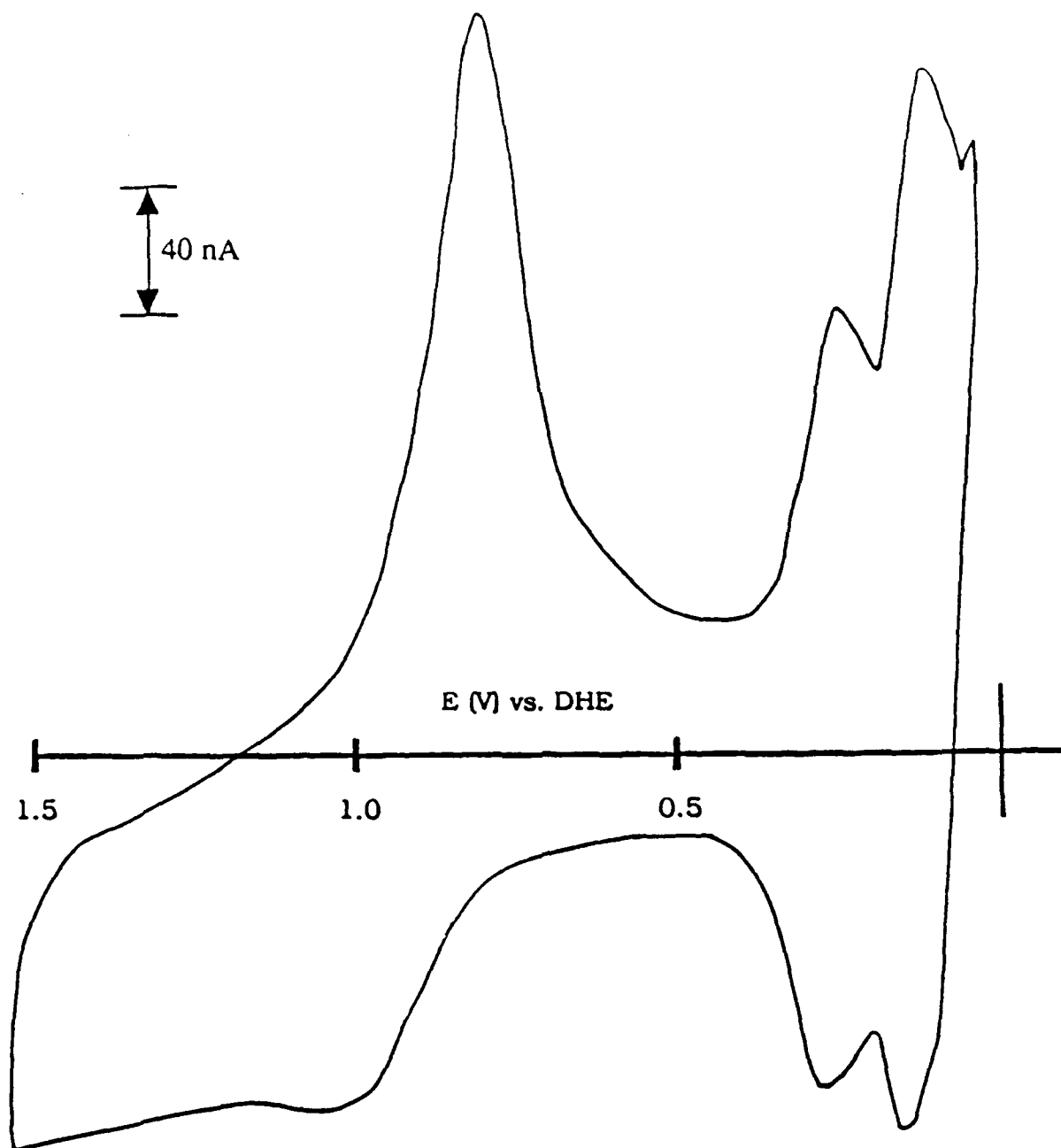


Figure 4

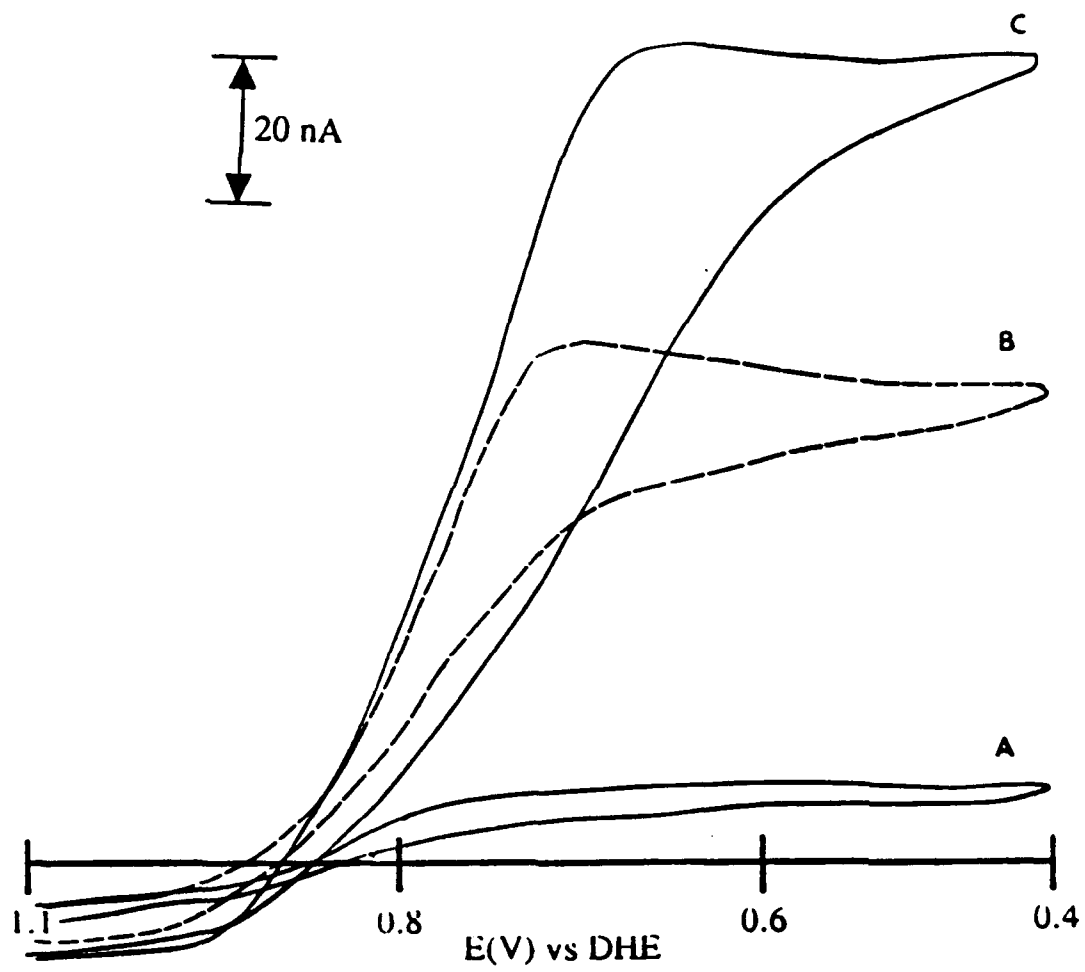


Figure 5

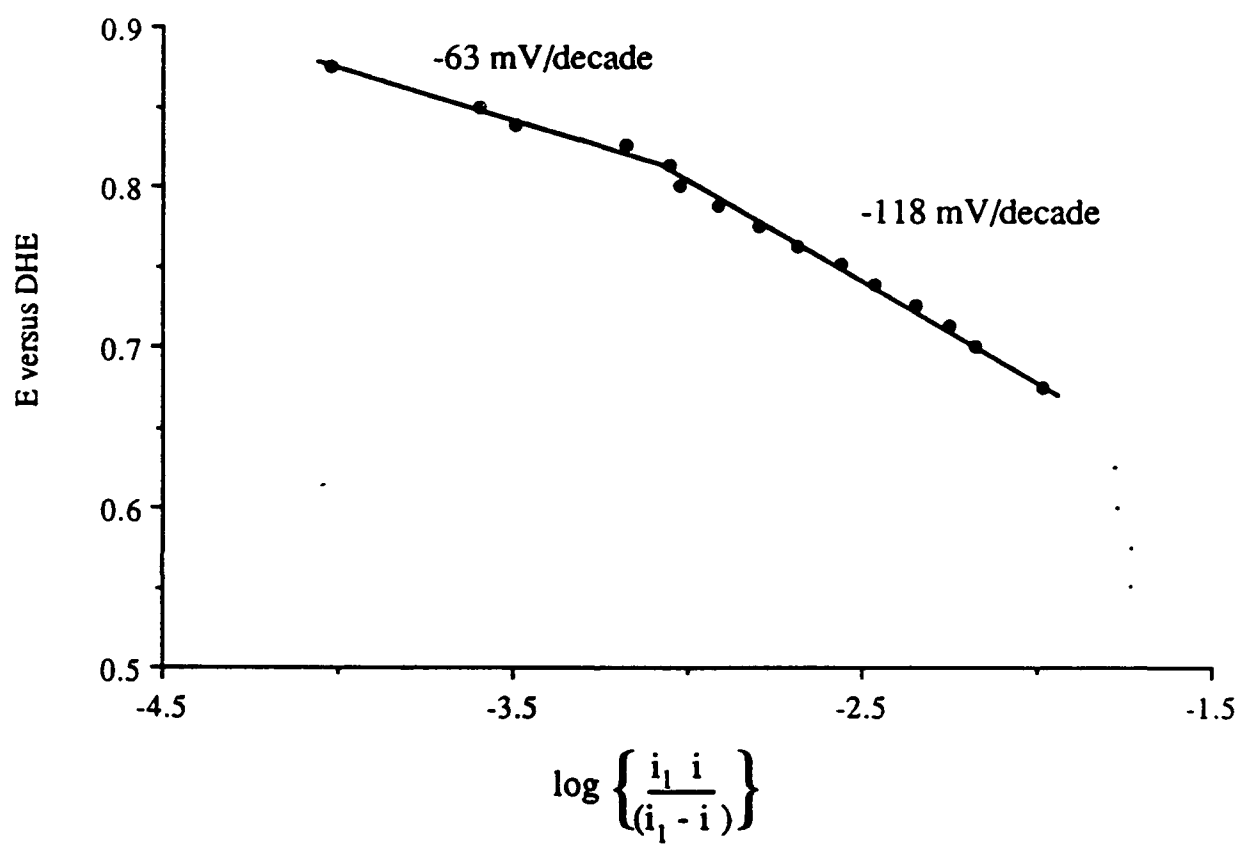


Figure 6



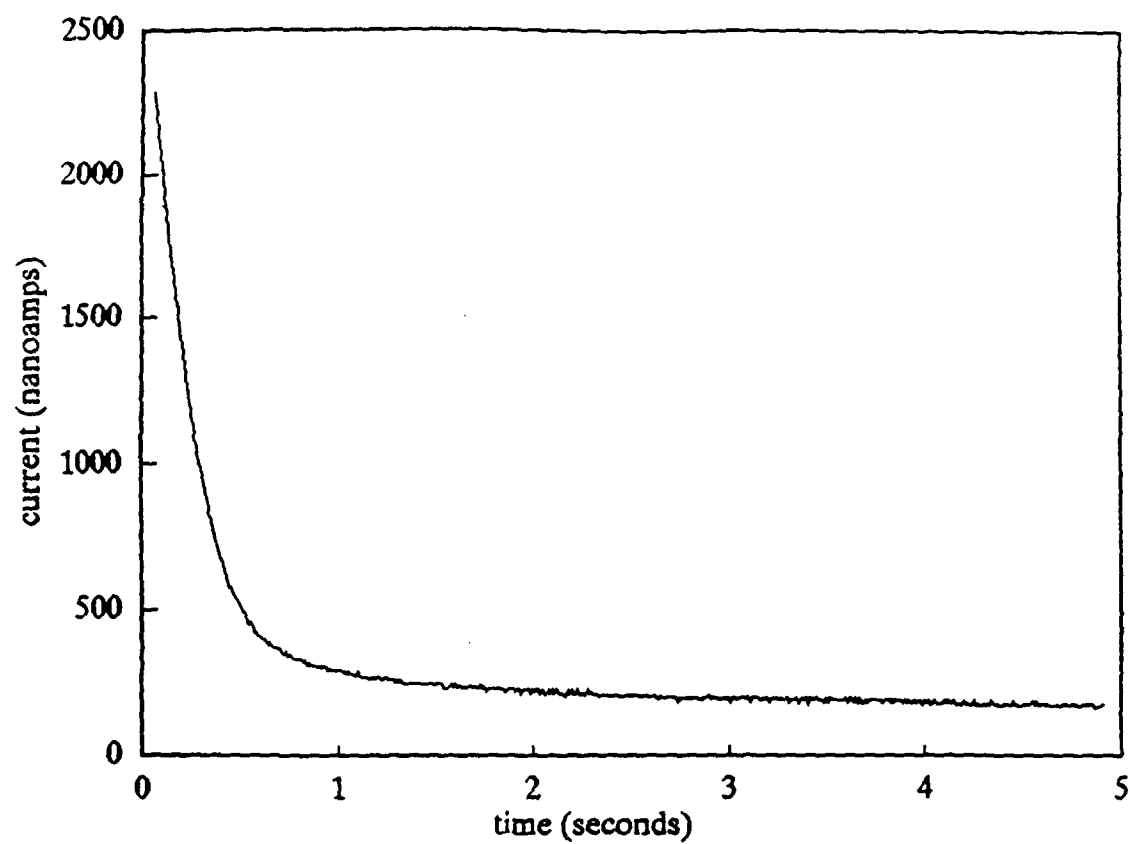


Figure 7

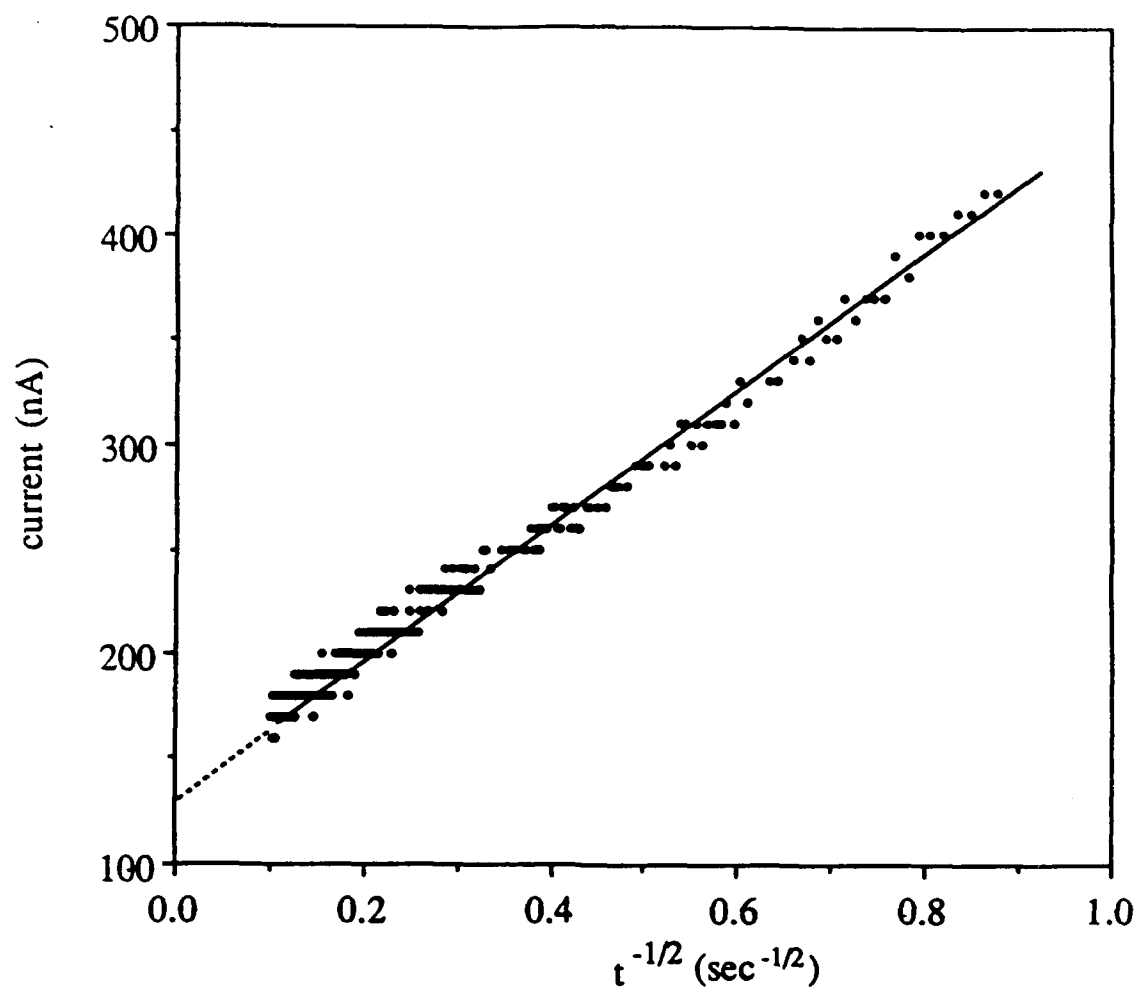


Figure 8